Model predictive control of wind turbine with aero-elastically tailored blades

R Hussain[1,2], H Yue[1] and L Recalde-Camacho[1]

[1] Wind Energy and Control Centre, Department of Electronic and Electrical Engineering, University of Strathclyde, 204 George Street, Glasgow, G1 1XW, UK
[2] Electrical Technology Section, Universiti Kuala Lumpur British Malaysian Institute, 53100 Gombak, Malaysia

E-mail: rohaida-binti-hussain@strath.ac.uk, hong.yue@strath.ac.uk, luis.recalde-camacho@strath.ac.uk

Abstract. The use of aero-elastically tailored blades (ATB) for large wind turbines has shown the benefit of mitigating blade loads, in a passive adaptive manner, with the design of bend-twist coupling (BTC) along the blades. The BTC design makes the blades torsionally flexible and capable of adapting to different wind speeds. However, such increased flexibility makes the turbine modeling computationally demanding and the real-time controller design more challenging. In this work, to include the ATB effect into the turbine model for control, a twofold modeling for ATB characteristics is proposed. First a static BTC distribution is added to the turbine aerodynamics to account for the blade's pre-bend-twist design, next a second-order transfer function is introduced to approximate the blade structural dynamic response to wind speed variations. The nonlinear model of the whole ATB wind turbine is built up in Simulink, linearized and discretized into a state-space form. A model predictive controller (MPC) is developed with the actuator constraints considered. Simulation studies are conducted on a 5MW ATB wind turbine at a selected above-rated wind speed. The use of the simplified model for control is assessed and the performance of MPC is compared to the gain-scheduling baseline controller.

1. Introduction

The demand for cleaner energy sources has pushed the developments of renewable technologies and particularly wind turbine technologies towards new engineering challenges. To produce more energy in a cost effective way, wind turbine rotors have become increasingly larger, leading to larger-size, heavier and more expensive blades. These blade designs are prone to bigger aerodynamic and inertial forces, and thus the need for mass-efficient turbines, capable of producing more energy is an ongoing research area.

1.1. ATB wind turbine modeling

Studies on improved blade performance focus mainly on reducing either weight or aerodynamic forces, see [1] and references therein. Weight reduction can be achieved by performing structural optimization of some or all of the turbine components. Alleviation of aerodynamic loads can be obtained by exploiting the capabilities of structural anisotropy and geometrical induced coupling at a cost of reduced annual energy production (AEP). In [2], Capuzzi et al. have shown new structural bend-twist coupling (BTC) concepts that suitably tailor the blade's elastic response

to aerodynamic pressure. Such blade designs increase the turbine's AEP while simultaneously alleviating loads. The blade BTC maximizes the energy extracted by adapting the angles of attack, along the blade length, to different wind speeds. The power extracted by these torsionally flexible blades thus depends on the total twist distribution, which can be represented as the sum of the pre-twist, the pitch angle regulated by a given controller and the elastically induced twist.

A comprehensive review of aero-elastically tailored blades (ATB) modeling and cross-sectional analysis can be found in [3]. There are very few ATB wind turbine modeling approaches, e.g. the geometrical approach to model an ATB wind turbine [4] and the blade model by [5] and [6]. An ATB model should contain an aerodynamic part to calculate the aerodynamic loads and a structural part to determine the structural dynamic response. For instance, in [2], Capuzzi et al. implement the blade structural model based on a finite element (FE) method, for an idealized and simplified blade. The aerodynamic modeling is carried out in an in-house Matlab model based on the Blade Element Momentum (BEM) theory with appropriate empirical corrections. Such models can be used for simulation and design analysis, but are not suitable for controller design. Simpler models for ATB wind turbines are required for development of control algorithms.

1.2. MPC for wind turbine control

Standard controllers for wind turbines are designed for torsionally rigid blades. At below rated wind speed operation, there is a single pitch angle and tip-speed ratio (TSR) that maximizes the turbine aerodynamic performance. At above rated wind speeds, pitch angle regulation suffices to keep the turbine operating at constant rated power, and the slowly varying nonlinear aerodynamics can be catered by gain-scheduling pitch regulation. This design approach is feasible since above rated aerodynamics can be assumed to vary independently on pitch angle and wind speed by means of aerodynamic separability [7].

For torsionally flexible blades, it can no longer be assumed that the maximum aerodynamic performance is achieved at a single TSR value [8]. The pitch activity will excite the blade motion and may cause flutter instability. Unlike the torsionally rigid blade, where flutter is not a problem, ATB turbines will have critical instability issues if the pitching is not properly controlled. This poses challenges for ATB wind turbine control. In [9], Recalde-Camacho et al. have shown that gain-scheduled controllers with additional load alleviation features may provide enhanced robustness to operate wind turbines with ATB. This, however, is based on the assumption that aerodynamic separability holds for ATB wind turbines, which is yet to be proven theoretically.

MPC has been widely used in many industries because of its ability to deal with multivariable systems, handle constraints and automatically cater for complexities such as non-minimum phase behaviors and time delays. MPC is an optimization problem that is solved at each sampling time to determine a finite sequence of control actions based on the predicted future outputs. A review of MPC for wind turbines is presented in [10]. Linear MPC is well established and is the preferred choice over nonlinear MPC since it requires less computational power. It has been proven that linear MPC can be designed to achieve desired power regulation and fatigue loads mitigation for industrial-scale wind turbines. Nonetheless, controller tuning requires careful parameter selection as wind turbines are highly nonlinear systems. The control performance can be further improved by using operating point scheduling and observers [10]. Adaptive MPC uses a fixed linear model structure but can adapt the prediction model for changing operating conditions, therefore suits for systems with strong nonlinear behaviors. To the authors' knowledge, MPC has not been used for wind turbines with ATB.

For pitch regulated wind turbines with ATB, hard constraints on pitch actuator can also be handled by MPC. The pitch actuator can only operate within its physical limits while the pitching rate should never exceed the ultimate limitations for safety reasons. A high pitching rate will risk the lifespan of the pitch actuator which increases the cyclic fatigue loading effect.

Exceeding these constraints may result in damage to the pitch actuators and ultimately the failure of the entire pitch control system [11].

In this work, an ATB wind turbine model is established including the aerodynamics with ATB, the rotor and tower structural dynamics approximation and the drive-train dynamics. The full nonlinear model is built up in Simulink, linearized and discretized into a linear state-space model, based on which MPC is developed. The remainder of this paper is organized as follows. Section 2 presents the modeling of ATB wind turbine that includes the static ATB characteristics and the dynamic ATB structural response approximation. Section 3 discusses the development of adaptive MPC for an ATB wind turbine. Simulation studies for a 5MW ATB wind turbine exemplar are presented in Section 4. The control performance is assessed for power production and load mitigation at a selected above-rated wind speed. Finally, conclusions are drawn in Section 5.

2. ATB wind turbine modeling

In this ATB wind turbine modeling, the aerodynamic loads are represented by the BEM equations, with the turbine aerodynamic coefficient calculated using DNV Bladed. The ATB structural dynamic part is approximated by a second-order transfer function model. The rotor and tower dynamics and the drive-train dynamics are represented by lumped parameter models. Key modeling details are presented in the following.

2.1. ATB feature static modeling

The main feature of an ATB in aerodynamics context is the bend and twist coupling, which is modeled in the aerodynamic subsystem of the turbine model as discussed in [12]. The BEM theory is applied to model a baseline wind turbine rotor first and then the model is modified by adding the ATB feature. The blade is divided into a number of sections and each section may have different airfoil profiles. The bend and twisting deformation is represented by adding the twisting angles to each blade section. This modification is integrated with the baseline BEM modeling for all blade sections. The aerodynamic force and the moment for each section provide the lift force and the moment for the entire blade. This ATB model is developed in DNV Bladed and it gives the static effect to the rotor performance caused by ATB.

Three ATB models were proposed for the twisting angles distribution in [13]. Model A is the blade design with a target twist angle distribution at the rated wind speed, Models B is enhanced with the finite element (FE) linear approach, and Model C is further enhanced by an FE nonlinear approach. More comparisons between the three ATB models for the 5MW baseline wind turbine can be seen in [12]. In this work, Model C is employed to represent the static ATB characteristics since it contains the nonlinear characteristics. Figure 1 and Figure 2 show the power coefficient and pitch angle variations over TSR using the 5MW baseline model.

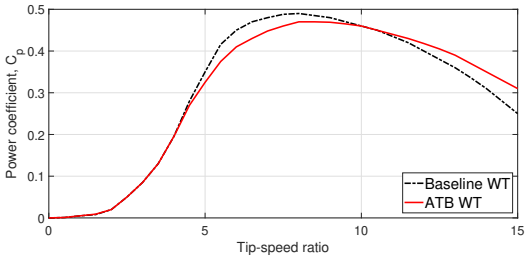

Figure 1. Power coefficient comparison

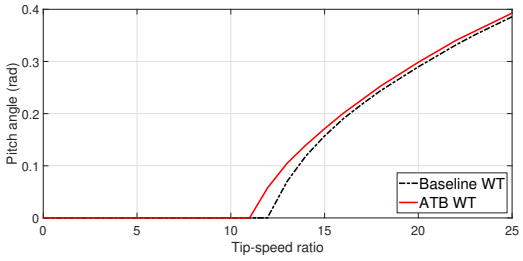

Figure 2. Pitch angle comparison

2.2. ATB structural response approximation

Based on the static ATB characteristics modeled using the BEM equations, a second-order model is introduced to approximate the ATB dynamics in the wind turbine model, written as the transfer function between the rotational displacement θ_{ATB} and the aerodynamic torque T_f.

$$G_{ATB}(s) = \frac{\alpha_{ATB}}{Js^2 + Ds + K} \tag{1}$$

This model is similar to a spring-mass-damper model, where K is the spring stiffness, J the moment of inertia and D the damping factor. α_{ATB} is the gain parameter kept for adjusting the scaling.

Effects of varying damping coefficient, spring stiffness and mass ratio were numerically examined in [14] for a semiactive flapping wing. The torsional stiffness of the segment can be expressed as

$$K = \frac{EA}{\Delta l} \tag{2}$$

where E is taken as the elastic Young's modulus of the blade root, A is the area of the cross section of the blade root and Δl is the length of the segment. Here the model in (1) is used to approximate the ATB structural response to wind speed variations, its parameters need to be determined for the specific turbine under study. In this work, the three parameters were firstly attempted for the 5MW baseline wind turbine as follows.

The Young's modulus for composite material is taken as $E = 72N/m^2$, the cross section area at the blade root is taken from DNV Bladed and is calculated with respect to the radius of $R = 0.41m$, which gives $A = 0.528m^2$. The length of the segment is taken as the distance from section 1 to section 2 along the blade (among the 19 divided sections counting from the root end), which is $\Delta l = 1.369m$. Therefore the torsional stiffness is calculated to be $K = 27.77N/m$ using (2).

In the 5MW baseline wind turbine structure, a single blade mass is $17,741kg$. The blade is divided into 19 sections making the mass for each section to be $933kg$ ($9152.73N$), the inertia is calculated to be $J = 900Nm^2$ for a radius of $0.31m$. The damping factor is chosen to be $D = 300$ to make the second-order transfer function model underdamped (with the damping ratio of 0.949).

Later on these model parameters are fine tuned to obtain the expected responses of the linearized turbine model at key frequency components, as shown in Figure 3. The tuned parameters are: $\alpha_{ATB} = 300$, $K = 30$, $J = 90$ and $D = 300$.

2.3. ATB wind turbine linearized model

Figure 4 shows a schematic representation of the wind turbine model with ATB, in which Ω_R is the rotor speed, Ω_G is the generator speed, T_d is the generator torque demand, β_d and β are the pitch demand and pitch angle applied to wind turbine, θ_{ATB} is the rotor in-plane displacement due to ATB, T_f is the aerodynamic torque.

The generator torque is assumed to be similar to torque demand since the power converter is relatively fast acting, and is defined to be equal to the rated generator torque as the controller is only tested at above rated wind speed values. The schematic figure also includes the pitch actuator dynamics since pitch angle constrains are considered in the MPC design.

The static ATB distribution is included in the aerodynamics subsystem, whereas the ATB dynamic response is supposed to act on the rotor dynamics by appropriately adjusting rotor in-plane displacement. The rotor is modeled by a single blade. In the inertial reference frame, the inertia of a single blade representation can be approximated by the inertia, about the axis of the low-speed shaft, of the complete rotor, and the stiffness is that required for the frequency to be the same for both the edge-wise and the flap-wise natural frequencies [15]. The rotor model

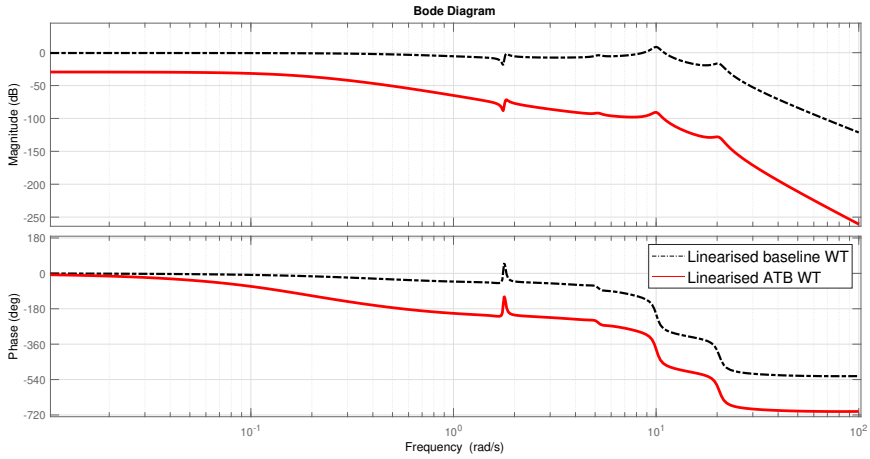

Figure 3. Bode plot for linearized model of baseline WT and ATB WT

is extended to include the dynamics of the components of the drive-train, that is, the hub, low speed shaft, gearbox, high speed shaft and generator. Simple spring-mass-damper models for each component are used since they are essentially linear. Such linear approximations introduce errors which are no larger than those implicit in the single blade representation and therefore allow a good approximation of the drive-train dynamics.

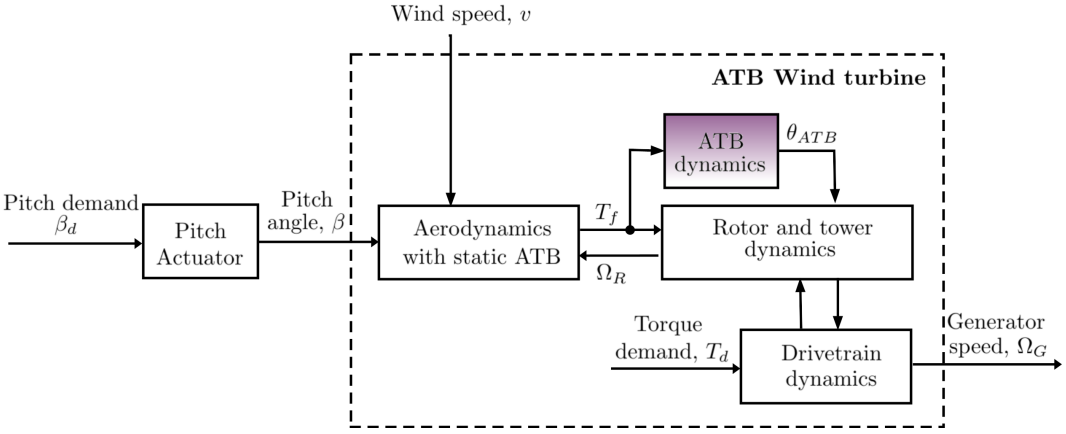

Figure 4. ATB wind turbine model schematic diagram

The turbine model in Figure 4 is first built up in Simulink which gives a nonlinear model. This nonlinear model is linearized and discretized into the following state-space form

$$\begin{aligned} x(k+1) &= Ax(k) + Bu(k) \\ y(k) &= Cx(k) \end{aligned} \tag{3}$$

where k is the time index, $A \in \mathbb{R}^{15\times15}$ and $B \in \mathbb{R}^{15\times1}$ are the parameter matrices for the state transition equation. The output parameter matrix is $C = [0_{14\times1}1]$.

The state vector x consists of 15 states, i.e.

$$x = \left[\theta_R, \Omega_R, \Omega_H, \theta_T, \dot{\theta}_T, \phi_R, \dot{\phi}_R, \phi_T, \dot{\phi}_T, \beta, \dot{\beta}, \theta_{ATB}, \dot{\theta}_{ATB}, \dot{\theta}_s, \Omega_G\right]^T.$$

These states represent key variables in the turbine model, which are listed in Table 1.

Table 1. State variables for the linearised model.

State	Variable name	Symbol
x_1	rotor displacement	θ_R
x_1	rotor speed	Ω_R
x_3	speed of hub	Ω_H
x_4	tower in-plane displacement	θ_T
x_5	tower in-plane speed	$\dot{\theta}_T$
x_6	rotor out-of-plane displacement	ϕ_R
x_7	rotor out-of-plane speed	$\dot{\phi}_R$
x_8	tower out-of-plane displacement	ϕ_T
x_9	tower out-of-plane speed	$\dot{\phi}_T$
x_{10}	pitch angle	β
x_{11}	pitching rate	$\dot{\beta}$
x_{12}	ATB in-plane displacement	θ_{ATB}
x_{13}	ATB in-plane speed	$\dot{\theta}_{ATB}$
x_{13}	equivalent low and high speed shaft displacement	θ_s
x_{14}	equivalent low and high speed shaft and gearbox speed	$\dot{\theta}_s$
x_{15}	generator speed	Ω_G

The control input is the pitch angle $u(k) = \beta(k)$, the output is the generator speed $y(k) = \Omega_G(k)$. This is a single-iput single-output model that is used for the controller design in Section 3. There are limited references if not none on ATB wind turbine dynamic system modeling. The model developed in this work can be taken as a working model for simulation and controller design.

3. Model predictive control of ATB wind turbine

3.1. Basic algorithm

A linear MPC is designed to control the wind turbine generator speed at a selected above rated wind speed. The optimization design problem at time k is formulated as

$$\min_{\Delta u(k)} J(k) = \sum_{i=1}^{n_y} e(k+i)^T Q e(k+i) + \sum_{i=0}^{n_u-1} \Delta u(k+i)^T R \Delta u(k+i) \tag{4}$$

$$\text{s.t.}$$
$$x(k+1) = Ax(k) + Bu(k)$$
$$u_{\min} \leq u(k) \leq u_{\max}$$
$$\Delta u_{\min} \leq \Delta u(k) \leq \Delta u_{\max}$$

where n_y is the output prediction horizon, n_u is the control horizon, and $n_u < n_y$. In (4), the first term penalizes the tracking error between the reference and the output,

$$e(k) = y(k) - r(k) \tag{5}$$

and the second term penalizes the incremental changes in the control input,

$$\Delta u(k) = u(k) - u(k-1) \tag{6}$$

Weights Q and R are used to compromise the trade off between the tracking error and the control cost. The constraints are applied to the control input, $u(k)$, which is the pitch angle, and its changing rate in $\Delta u(k)$. At each time k, the constrained optimization problem is solved with the quadratic programming (QP) method to give the control sequence over the control horizon n_u, and the fist control signal in this sequence is applied to the system [16].

3.2. Control system configuration

The control system block diagram with MPC is shown in Figure 5. The linearized MPC is designed based on the linearized state-space model and the control action is applied to the nonlinear wind turbine model. When the controller is used to regulate wind turbine generator speed across the full range of above rated wind speeds, adaptive MPC is required to compensate for the mismatch between the linearized model in MPC and the nonlinear wind turbine model. Model update and Kalman filter are introduced for such purpose. The model update can be made by methods such as recursive least square parameter estimation, neural-network based tuning, normally conducted in a larger time scale than the sampling time for control. For simulations of turbulent wind speed, with a set mean value, the nonlinear dynamics are slowly varying and a combination of Kalman filter and MPC suffices. With this design scheme, the computational demand for real-time optimization is reduced compared to using nonlinear MPC, while the control performance is not compromised by the linear control.

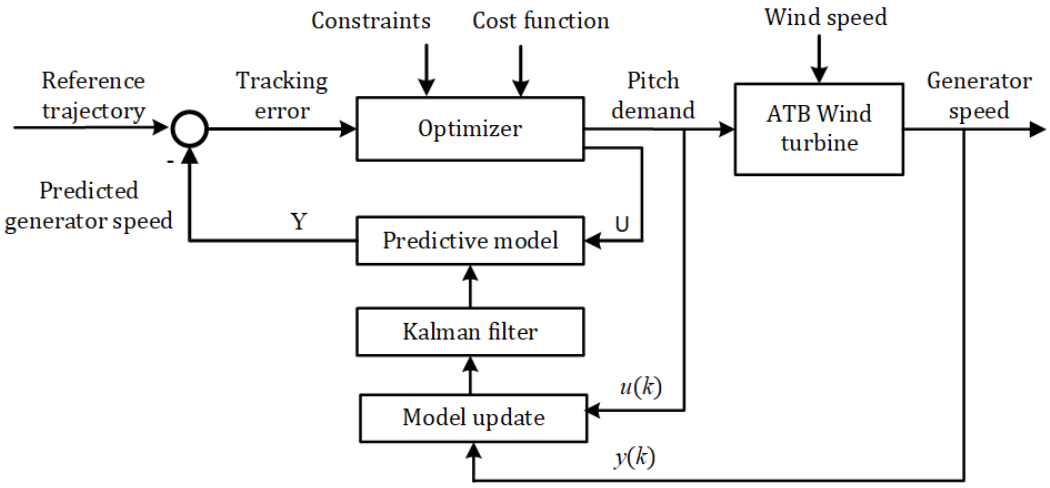

Figure 5. Block diagram for ATB wind turbine with MPC

The MPC solution requires the estimated states at each time k, for which a steady-state Kalman filter is designed. The Kalman filter equations are

$$\begin{aligned} \hat{x}(k+1|k) &= A\hat{x}(k|k-1) + Bu(k) + L\left(y(k) - \hat{y}(k)\right) \\ \hat{y}(k) &= C\hat{x}(k|k-1) \end{aligned} \tag{7}$$

where $\hat{x}(k|k-1)$ is the model estimated states, $\hat{y}(k)$ is the linearised model output and $y(k)$ is the nonlinear model output. The Kalman gain L is derived by solving a discrete Riccati equation.

4. Simulation study

4.1. Computational set-up

The developed ATB wind turbine model and the MPC algorithm are simulated on a 5MW variable speed pitch regulated horizontal axis wind turbine exemplar system, implemented in

Simulink. The wind turbine specifications are given in Table 2. The baseline turbine model has been modified using the developed ATB model as discussed in Section 2. The BEM equations are used to calculate turbine aerodynamics with turbine aerodynamic coefficient being calculated with DNV Bladed. The simulation is carried out for above rated wind speed of magnitude 16m/s with turbulence intensity of 10%. With the selected mean wind speed and the level of turbulence intensity, the stochastic component of the wind speed will be sufficiently large to produce a significant bend and twist blade response and therefore suits the testing of the controller adaptation.

In control simulations, the developed MPC is compared against a gain-scheduled baseline controller given by the following transfer function:

$$C(s) = \frac{K_{GS}(\beta) \cdot K \cdot (s+z)}{s(s+p)} \tag{8}$$

The controller has a constant gain K, a variable gain scheduled in pitch angle $K_{GS}(\beta)$, an integrator to remove the steady-state tracking error and a phase-lag compensator, with zero z and pole p such that it speeds up system's response and increases system's stability, i.e $p > z$.

The MPC parameters are tabulated in Table 3. In this work, single input (pitch angle) and single output (generator speed) control is considered. In the performance function in (4), the weighting factor for the tracking performance is set to be $Q = 1$ and the weight for the control cost is tuned to be $R = 2$ to make a balanced trade off. The sampling time for discretization and control is 0.2s. The model prediction horizon and the control horizon are set to be $n_y = 20$ and $n_u = 5$. All simulations are run over a 10-minute time range.

Regarding the actuator constraints, the lower bound for the pitch angle is 0 rad and the upper bound is 0.3 rad. A suggested value of 10 deg/s applies to pitching rate constraint as a common practice in wind turbine control [10], which is equivalent to 0.035 rad using our definition of $\Delta u(k)$ in (6) (1 deg = 0.01745 rad, $T_s = 0.2s$). In this simulation, the pitching rate constraint is set between -0.01 and 0.01 rad, which is a tighter constraint compared to the commonly used one.

Table 2. Wind turbine specifications.

Parameter	Value
Rated power	5MW
Rotor diameter	63m
Hub height	90m
Rated generator speed	120rad/s
Rated generator torque	46,372Nm

Table 3. MPC parameters.

Parameter	Value
Sampling time	0.2s
Simulation time	600s
Prediction horizon	20
Control horizon	5
Pitch angle constraint	$[0, 0.3]$rad
Pitching rate constraint	$[-0.01, 0.01]$rad
Weighting factors	$Q = 1, R = 2$

The wind speed time series are also generated using DNV Bladed. In the IEC 61400 standards it is suggested to run at least six 10-minute stochastic realizations to ensure statistical reliability of the simulation. In the simulation, six different stochastic realizations of the 16m/s wind speed have been used, each time series is 600s long, see Figure 6.

4.2. Simulation results

Simulations are made for the selected wind speed in 6 seeds. In all the comparisons, two sets of results are provided, one is the MPC control for the ATB wind turbine model, the other one

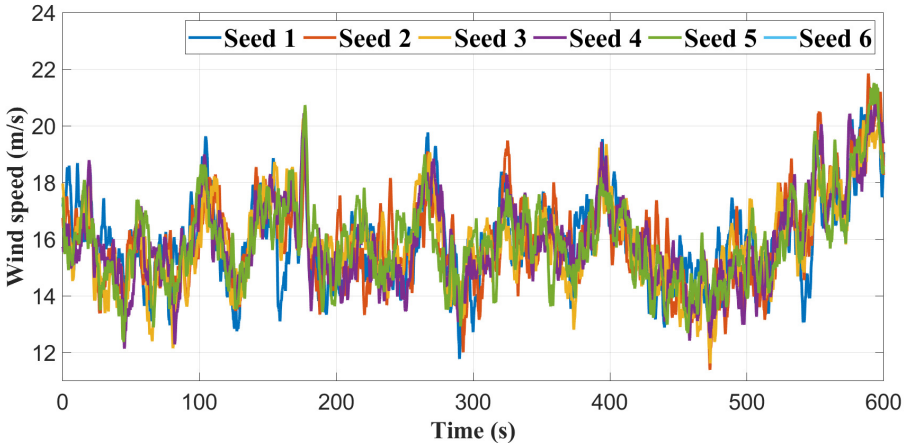

Figure 6. Wind speed variation at 16 m/s for 6 seeds

is the baseline gain-scheduling (GS) control for the baseline rigid-blade turbine model without ATB.

The results of the pitch angle variance and the generator speed variance are summarized in Table 4. It can be seen that the MPC controller reduces the variance in generator speed, thus achieving a smoother regulation, and most importantly, without significantly increasing the pitch activity. These results are consistent throughout the six different wind speed stochastic realizations. During simulation, Seed 2 also showed higher standard deviation thus increasing pitch activity for both controllers. In the following results, one wind speed stochastic realization (Seed 1) is selected to simplify the illustration.

Table 4. Above rated control results at 16m/s wind speed (6 seeds).

Variance	**Pitch variance**		**Generator speed variance**	
Wind speed seeds	**Baseline**	**MPC**	**Baseline**	**MPC**
Seed 1	0.0017	0.0022	33.49	21.59
Seed 2	0.0022	0.0043	33.67	32.53
Seed 3	0.0015	0.0032	33.93	24.36
Seed 4	0.0013	0.0027	34.22	22.16
Seed 5	0.0018	0.0033	33.36	24.58
Seed 6	0.0017	0.0027	34.35	23.66

Figures 7 and 8 show the power spectral density (PSD) curves of the power output and the tower fore-aft root bending moment, respectively. Two sets of results are presented. One is the rigid blade baseline turbine under the baseline gain-scheduling controller (black line) and one is the ATB turbine with MPC (red line).

The power PSD from Figure 7 shows an increase in energy when the rigid-blade baseline turbine is controlled with the baseline gain-scheduling controller. MPC for ATB turbine brings down the energy level slightly which translates into smoother regulation of power. In the tower root bending moment PSD plot (Figure 8), the application of constraints in MPC reduces the energy required for pitch regulation activity. The peak visible in the red line, slightly over 2

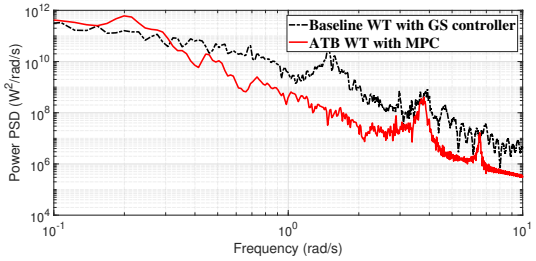

Figure 7. PSD for power output

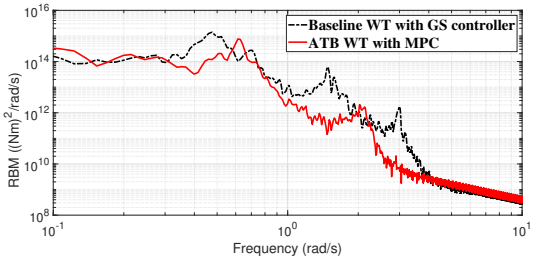

Figure 8. PSD for tower RBM

rad/s, is a by-product of the feedback sensitivity transfer function which causes an energy lobe at the right of the tower frequency (waterbed effect).

Further simulation results are assessed in time domain on the pitch angle, the incremental change of pitch angle (pitching rate), the generated power and the tower fore-aft root bending moment for the MPC controlled ATB turbine and the gain-scheduling controller baseline turbine (the one without ATB). Results are presented in Figures 9 – 14.

Figure 9 shows pitch angle time profiles and Figure 10 presents the result for Δu. It can be observed that the constrains for u and Δu are both satisfied for MPC. The results in Figure 9 and Table 4 suggest that the ATB wind turbine under MPC has a smaller variation in pitch activity as compared to the rigid blade baseline turbine under the baseline gain-scheduling control. Also, lower pitching rate has the advantage to increase the lifespan of the ATB wind turbine system.

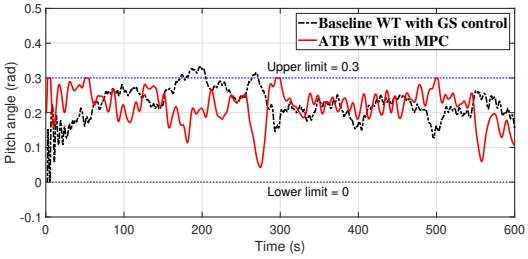

Figure 9. Pitch angle (u) with MPC and baseline gain-scheduling control

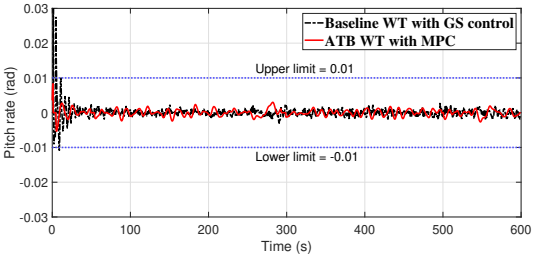

Figure 10. Pitch rate (Δu) with MPC and baseline gain-scheduling control

Figure 11 and Figure 12 show the power output and the generator speed time profiles. The two sets of results are close to each other. The output power varies around the rated power of 5MW with the variance proportional to the generator speed as present in Table 4. The mean value for the output power under MPC is 4.96 MW. This result is tolerable as it is within a 99% range around the expected rated power.

Figure 13 shows the tower fore-aft acceleration, from which it can be seen that the tower acceleration is smaller for the MPC controlled ATB wind turbine. Figure 14 shows the tower fore-aft root bending moment. In the first stage of the simulation (see the first 100 seconds in Figure 14, the tower's root bending moment under MPC has a much smaller variation. This improvement over the rigid-blade turbine under baseline control is partly due to the MPC's optimization at each time instance, and partly due to the ATB characteristics.

5. Conclusions

Model predictive control of industrial-scale wind turbines with ATB design are explored in this work. A key challenge tackled is the development of a working model for such systems.

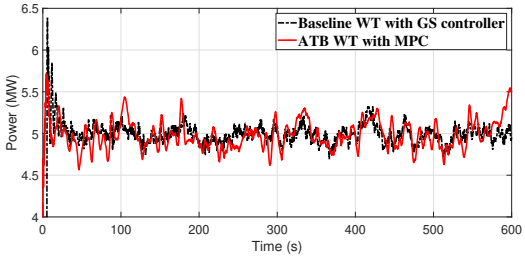

Figure 11. Power output with MPC and baseline gain-scheduling control

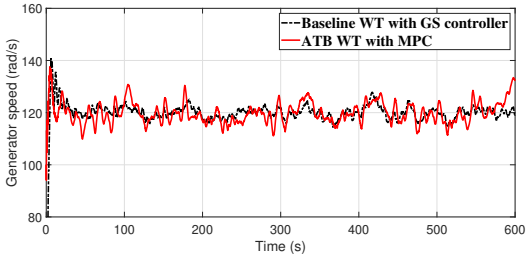

Figure 12. Generator speed with MPC and baseline gain-scheduling control

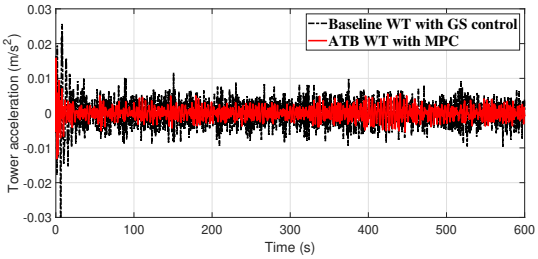

Figure 13. Tower acceleration with MPC and baseline gain-scheduling control

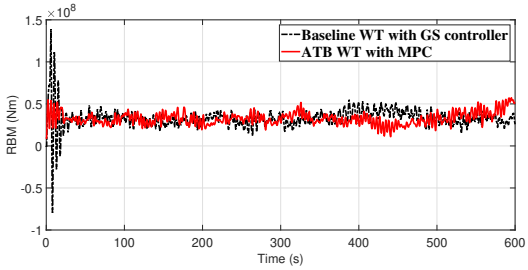

Figure 14. Root bending moment with MPC and baseline gain-scheduling control

No existing models are found available for real-time controller design purpose. We propose to establish the ATB wind turbine model in several steps. In the first step, the BTC distribution is introduced to the aerodynamic model block using a static design taken from literature. In the second step, the structural dynamics of the ATB are approximated by a second order transfer function. In this way, the dynamic ATB characteristics is captured without expensive computational demands. The developed nonlinear model including other subsystems is then linearized and discretized for controller design.

Another challenge is to control the ATB wind turbine that has more complexity where the aerodynamic separability for rigid-blade turbines may not apply. Linear MPC is chosen considering its powerful function of receding-horizon optimization and convenient handling of constraints. Controller tuning of MPC is conducted to achieve the balance between the tracking performance and the control cost. In order to assure reliable analysis, six different stochastic realizations of a selected above-rated wind speed are used in the numerical test. The control results of MPC for the ATB turbine are compared with a baseline gain-scheduling controller for the rigid-blade turbine on a number of metrics such as PSD of the generator speed and the root bending moment in frequency domain, pitching control activities, generated power and root bending moment in time domain. Consistent performance improvement can be observed for MPC in that the load mitigation is achieved without compromising the power generation and increasing the control activities.

The current results are obtained from a selected above-rated wind speed. The MPC strategy needs to be further tested under wider wind speed variations, where the model update is required in the adaptive MPC scheme. For the same reason, the linearized ATB wind turbine model is yet to be validated over the full range of wind speeds, e.g. whether the common features at crucial frequencies can be reliably captured.

Acknowledgements
This research was partly funded by UK EPSRC through the Centre for Doctoral Training in Wind and Marine Energy Systems at the University of Strathclyde (no. EP/L016680/1). This work is partly supported by Malaysian Government Agency, Majlis Amanah Rakyat (MARA) and Universiti Kuala Lumpur.

References
[1] Capuzzi M, Pirrera A and Weaver P 2014 *Energy* **73** 15–24
[2] Capuzzi M, Pirrera A and Weaver P 2014 *Energy* **73** 25–32
[3] Wang L, Liu X and Kolios A 2016 *Renew. Sust. Energ. Rev.* **64** 195–210
[4] Wang L, Liu X, Renevier N, Stables M and Hall G M 2014 *Energy* **76** 487–501
[5] Baumgart A 2002 *J. Sound Vib.* **251** 1–12
[6] Li L, Li Y, Liu Q and Lv H 2014 *Appl. Math. Model.* **38** 2695–2715
[7] Leithead W, Leith D, Hardan F and Markou H 1999 Global gain-scheduling control for variable speed wind turbines *EWEC-CONFERENCE* pp 853–6
[8] Scott S, Capuzzi M, Langston D, Bossanyi E, McCann G, Weaver P M and Pirrera A 2017 *Renew. Energ.* **114** 887 – 903
[9] Recalde-Camacho L, Stock A and Giles A D 2020 Control of aeroelastically-tailored wind turbines Tech. rep. University of Strathclyde
[10] Lio W H, Rossiter J and Jones B L 2014 A review on applications of model predictive control to wind turbines *2014 UKACC Int. Conf. Contr. (Control)* (IEEE) pp 673–8
[11] Liu Y, Ferrari R M and van Wingerden J W 2021 *arXiv preprint arXiv:2104.04250*
[12] Hussain R, Yue H, Leithead W and Xiao Q 2017 *IFAC-PapersOnLine* **50** 10342–10347
[13] Capuzzi M, Pirrera A and Weaver P M 2015 *Thin-Walled Struct.* **95** 7–15
[14] Zhu J 2019 *Int. J. Aerosp. Eng.* **2019**
[15] Leithead W E and Rogers M 1996 *Wind Eng.* **20** 149–174
[16] Buijs J, Ludlage J, Van Brempt W and De Moor B 2002 *IFAC Proc. Volumes* **35** 301–306